Building Services Engineering Research and Technology
http://bse.sagepub.com/

Building instantaneous cooling load fused measurement: multiple-sensor-based fusion versus chiller-model-based fusion

Gongsheng Huang, Yongjun Sun and Shengwei Wang

BUILDING SERV ENG RES TECHNOL 2013 34: 177 originally published online 11 January 2012
DOI: 10.1177/0143624411432651

Article

BUILDING SERVICES ENGINEERING RESEARCH & TECHNOLOGY

Building Serv. Eng. Res. Technol.
34(2) 177–194

DOI: 10.1177/0143624411432651
bse.sagepub.com
SAGE

Building instantaneous cooling load fused measurement: multiple-sensor-based fusion versus chiller-model-based fusion

Gongsheng Huang[1], Yongjun Sun[2] and Shengwei Wang[2]

Abstract

Building instantaneous cooling load is an essential variable for the optimisation and supervisory control of chiller plants, which can be estimated according to the measurements of the chilled water flow rate and the chilled water temperature drop through the chiller plants. Since the measurements of the flow rate and the temperature drop suffer from measurement uncertainties, two different fusion approaches have been developed to improve the measurement accuracy of the cooling load. One is the chiller-model-based fusion (CMF) approach and the other is the multiple-sensor-based fusion (MSF) approach. The two approaches use different disciplines to fuse available measurements. This paper describes a comparison study of the two fusion approaches, which analyses the influences of cooling load conditions of chiller plants on the performance of the two approaches. A case study based on computer simulation shows that the CMF approach is able to produce a better result when the cooling load condition is relatively stable and redundant measurements of the chilled water temperature and flow rate are deficient; while when the redundant measurements are abundant the MSF approach can produce a better result.

Practical applications: The study aims to identify the advantage/disadvantage of two fusion approaches proposed for improving the accuracy of building cooling load measurement under different load conditions. For practical applications, results may be used as a guideline for selecting a proper fusion approach for a particular chiller plant according to the characteristics of its actual load condition.

Keywords

Building instantaneous cooling load, data fusion, measurement uncertainty, redundant measurement

Introduction

Building instantaneous cooling load is widely used in chiller plant supervisory control and optimisation for improving the energy efficiency of chiller plants,[1,2] and becomes an important

[1]Building Energy and Environmental Technology Research Unit, Division of Building and Science, City University of Hong Kong, Kowloon, Hong Kong
[2]Department of Building Services Engineering, Hong Kong Polytechnic University, Kowloon, Hong Kong

Corresponding author:
Yongjun Sun, Department of Building Services Engineering, Hong Kong Polytechnic University, Kowloon, Hong Kong.
Email: beyjsun@polyu.edu.hk

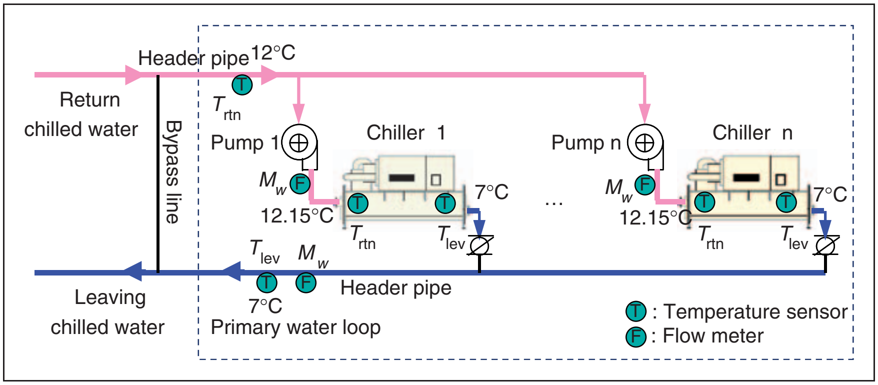

Figure 1. A typical multiple-chiller plant

measurement for building energy management systems. For example, it is used in chiller sequencing control to determine chiller staging on-off operation,[2,3] in chilled water temperature optimisation to estimate the optimal chilled water supply temperature,[2,4] and in chiller fault detection and diagnosis to monitor the health of chiller plants.[5] In chiller plant supervisory control and optimisation, the building of instantaneous cooling load is usually estimated according to the chilled water temperature differential and the mass flow rate by Equation. (1),[6] where the temperature and flow rate are measured at the header pipes of chiller plants as shown in Figure 1. This cooling load estimation is titled as cooling load direct measurement:

$$Q_{dm} = \dot{m}_w \rho_w (T_{rtn} - T_{lev}). \quad (1)$$

In order to acquire accurate cooling load, the accuracy of the flow meter and temperature sensors is required to be as high as possible, especially the sensors for the chilled water return and leaving temperature. This is because the differential between the chilled water leaving temperature T_{lev} and the return temperature T_{rtn} is normally 3°C to 5°C. Uncertainties in the temperature measurements have a significant influence on the measurement accuracy of the cooling load. For example, if T_{rtn} diverges from its true value by 0.2°C and T_{lev} by −0.2°C, the cooling load will diverge from its true value by nearly 10%. This can explain why two set of sensors were used to measure the chilled water temperature differential and the differences between the two measurements were over 30% in a large proportion.[7]

Commonly used flow meters for chilled water plant control application are of the electromagnetic and ultrasonic type. Both types can provide accurate reading. Since there are no sensing components that interrupt the flow path and they are mounted externally to existing pipelines, little maintenance is involved in both meters.[8,9] However, places where ultrasonic sensing can be installed are frequently limited, since at least a 1 m straight section of pipe is often required, which may be often difficult to find in practice. Another problem is the turbulent flow since the measured flows are turbulent in most applications. Although ultrasonic sensing has advanced to a level of accuracy where the turbulence of the measured media is the main source of fluctuations in the measured flow value,[10] the condition with the minimum of turbulence is still preferred in order to avoid fluctuations in measurement. Similar problems exist for the electromagnetic type. A minimum of 10 pipe diameters of straight run upstream and 5 diameters downstream is recommended; and some situations may require even 20 pipe diameters or more upstream to ensure a fully developed turbulent flow profile.[11]

Inappropriate installation of flow meters will degrade the quality of the measurement. Thermistors and resistance temperature detectors (RTDs) are the most common devices used for temperature measurement in chiller plants. In applications, indirect stainless-steel well temperature sensors are always employed so that the sensor can be removed conveniently from the well for calibration or test.

In practice, however, it has been found that the cooling load estimated by Equation (1) is not always accurate and stable.[12] The overall accuracy of the measurements is not only determined by the accuracy of the sensors, but also by that of the transmitter as well as the communication network that are used to transport the measurements. In chiller plants, the measurement tools and the communication networks are generally working under noisy and vibrating conditions due to the operation of chillers and pumps. External disturbances affect the signal transmission and the data collection. Therefore, even if the sensors are of high accuracy (which is not always true in building systems due to the low-cost nature[13]), the overall accuracy of the measurements may still not be acceptable.[8] Except for the measurement accuracy, the quality of the measurements is also influenced by the characteristics of measurands. In the cooling load estimation by Equation (1), the precision will be low if the distribution of the chiller water flow rate and temperature is uneven or unstable in a large pipe, which will cause fluctuations in the measurements.

According to their principle of generation, measurement uncertainties are usually categorised into noise, outlier and bias. Measurement uncertainties may cause the optimisation and supervisory control to become meaningless. They may also cause the control system unstable. For example, until now the variable time-delay in sensing systems is a challenging issue in the control design and how to deal with the variable time-delay in control design is still a hot research topic.[14,15] In order to reduce the magnitude of uncertainties in cooling load measurements, two approaches have been developed. One is the chiller-model-based fusion (CMF) approach[12] and the other is the multiple-sensor-based fusion (MSF) approach.[16] At the first step, the CMF approach uses an inverse chiller model to calculate the cooling load according to the power consumption, the condensing, and the evaporating pressure of the chiller. This cooling load calculation is titled as cooling load indirect measurement in this paper. Then, the indirect measurement is used to calibrate the direct measurement.

The MSF approach fuses redundant measurements of the chilled water return temperature, leaving temperature and flow rate individually at the beginning. Here redundant measurements refer to data from different sources but measuring a same variable. In chiller plants, when operating chillers can provide the measurements of the chilled water return temperature, the leaving temperature and the flow rate, those data are redundant correspondingly with the measurements at the header pipes, which is shown in Figure 1. Then, the fused measurements are used to calculate the cooling load by Equation (1) instead of the measurements at the header pipes.

The two approaches use different disciplines to improve the accuracy of the cooling load measurement. It is necessary to compare the performance of the two approaches. This paper describes a comparison study of the two fusion approaches under different operating conditions. The comparison study is performed with the aid of TYNSYS, a professional software to simulate the transient behaviour of HVAC systems.[17] Results show that the CMF approach is able to produce a better result when the cooling load condition is relatively stable and redundant measurements of the chilled water temperature and flow rate are deficient; while when the redundant measurements are abundant the MSF approach can produce a better result.

Description of the two fusion approaches

Considering measurement noises and biases, the measurements of the chilled water leaving and return temperatures and the flow rate can be written as Equations (2), (3) and (4), respectively, where the noises are assumed to follow normal distributions with zero expectation and the biases are assumed to be unknown constants. When the measurements of chilled water return temperature, leaving temperatures and flow rate are independent, the cooling load calculated by Equation (1) has the form of Equation (5), where e_{dm} follows a normal product distribution. It should be noted that outliers are not included in the description of the following equations:

$$T_{\mathrm{rtn,\,hd},\,k} = T_{\mathrm{rtn,\,act},\,k} + e_{\mathrm{rtn,\,hd},\,k} + b_{\mathrm{rtn,\,hd}},\; e_{\mathrm{rtn,\,hd}} \sim N\left(0, \sigma^2_{\mathrm{rtn,\,hd}}\right) \tag{2}$$

$$T_{\mathrm{lev,\,hd},\,k} = T_{\mathrm{lev,\,act},\,k} + e_{\mathrm{lev,\,hd},\,k} + b_{\mathrm{lev,\,hd}},\; e_{\mathrm{lev,\,hd}} \sim N\left(0, \sigma^2_{\mathrm{lev,\,hd}}\right) \tag{3}$$

$$\dot{m}_{w,\,\mathrm{hd},\,k} = \dot{m}_{w,\,\mathrm{act},\,k} + e_{w,\,\mathrm{hd},\,k} + b_{w,\,\mathrm{hd}},\; e_{w,\,\mathrm{hd}} \sim N\left(0, \sigma^2_{w,\,\mathrm{hd}}\right) \tag{4}$$

$$Q_{\mathrm{dm},\,k} = Q_{\mathrm{dm,\,act},\,k} + e_{\mathrm{dm},\,k} + b_{\mathrm{dm}}. \tag{5}$$

Chiller-model-based fusion approach

The CMF approach uses an indirect measurement of the cooling load to calibrate the direct measurement. The indirect measurement is denoted as Q_{im} and calculated by Equation (6), where N is the total number of the operating chillers and $Q_{\mathrm{im},i}$ indicates the cooling load of the ith operating chiller, which is derived using an inverse chiller model as described by Equations (7) and (8):[18]

$$Q_{\mathrm{im},\,k} = \sum_{i=1}^{N} Q_{\mathrm{im},\,i,\,k} \tag{6}$$

$$Q_{\mathrm{im},\,i,\,k} = \frac{W_{\mathrm{ch},\,i,\,k} - \beta_i}{(1+\alpha_i)\Delta h_{i,\,k}} \times (cp_l \times T_{\mathrm{cd},\,i,\,k} - h_{\mathrm{fg}} - cp_g \times T_{\mathrm{ev},\,i,\,k}) \tag{7}$$

$$\Delta h_{i,\,k} = r\zeta T_{\mathrm{ev},\,i,\,k} \frac{\gamma}{\gamma-1}\left[\left(\frac{P_{\mathrm{cd},\,i,\,k}}{P_{\mathrm{ev},\,i,\,k}}\right)^{\frac{\gamma-1}{\gamma}} - 1\right] \Big/ 1000. \tag{8}$$

Since this model is derived using an ideal refrigerant cycle, model errors exist even if the parameters α_i and β_i are identified by considering full and part load conditions. According to experimental and simulation studies, the model errors are usually within 10%.[18,19] Using δ_{im} to denote the measurement error due to the model mismatch, the indirect measurement is rewritten as

$$Q_{\mathrm{im},\,k} = Q_{\mathrm{act},\,k} + \sum_{i=1}^{N} \delta_{\mathrm{im},\,i,\,k} = Q_{\mathrm{act},\,k} + \delta_{\mathrm{im},\,k}. \tag{9}$$

The size of the measurement mismatch is relative to the cooling load condition, that is, δ_{im} has a different value when Q_{act} is different. Also the dynamics between Q_{im}, P_{cd}, P_{ev} and Q_{act} will affect the indirect measurement since the inverse chiller model described by Equations (7) and (8) is a static model. This dynamics becomes less significant when the cooling load condition is stable. In this situation, the model mismatch δ_{im} can be efficiently removed using the incremental form of Equation (9) as shown by

$$\Delta Q_{\mathrm{im},\,k} \approx \Delta Q_{\mathrm{act},\,k}. \tag{10}$$

The basic fusion formula used in the CMF approach is

$$Q_{f,\,k} = \frac{1}{N}\sum_{i=1}^{N} Q^{\kappa}_{\mathrm{dm},\,i} + \frac{1}{N} A^t \Pi_{\mathrm{im},\,k} \tag{11}$$

where k indicates the current time instant; i is the ith data in the moving window; N is the horizon of the moving window; κ indicates the current moving window; $A^t = [N-1, \ldots, 1]$; and $\Pi_{\mathrm{im},k}$ is defined by

$$\Pi_{\mathrm{im},k} = \left[\Delta Q^{\kappa}_{\mathrm{im},N}, \ldots, \Delta Q^{\kappa}_{\mathrm{im},2}\right] \quad \text{with}$$
$$\Delta Q^{\kappa}_{\mathrm{im},i+1} = Q^{\kappa}_{\mathrm{im},i+1} - Q^{\kappa}_{\mathrm{im},i}, i = 1, \ldots, N-1.$$

In formula (11), the first right-hand side (RHS) item is the average value of the direct measurements in the moving window that is used to reduce the measurement noises. Since the measurement noises follow a normal distribution with zero expectation, the noise reduction depends on the length of the moving window. By statistics theory, a longer moving window will lead to a better noise reduction. The second RHS item is the calibrator, which uses the weighted average increments of the indirect measurements: the newer measurements have a larger weight. The use of the increments aims to reduce the influence of the model mismatch δ_{im}.

The structure of the CMF approach for the multiple-chiller plant is illustrated in Figure 2. The CMF approach has the functions of detecting (and removing) outliers and detecting (and reducing) biases in the direct measurements in order to improve the reliability of the fused measurements. It also evaluates the confidence degree of the fused measurements. The details are given in Appendix A for self-consistency.

Multiple-sensor-based fusion approach

The MSF approach fuses redundant measurements available in chiller plants. Assume there are M redundant measurements on the variable x at the current time instant k. The basic fusion formula is

$$x_{m,k} = \sum_{i=0}^{M_k} \lambda_{i,k} x_{i,k} \quad \text{with} \quad \lambda_{i,k} = \frac{\prod_{j=0,j\neq i}^{M_k} U^2_{j,k}}{\sum_{i=0}^{M_k}\left[\prod_{j=0,j\neq i}^{M_k} U^2_{i,k}\right]} \tag{12}$$

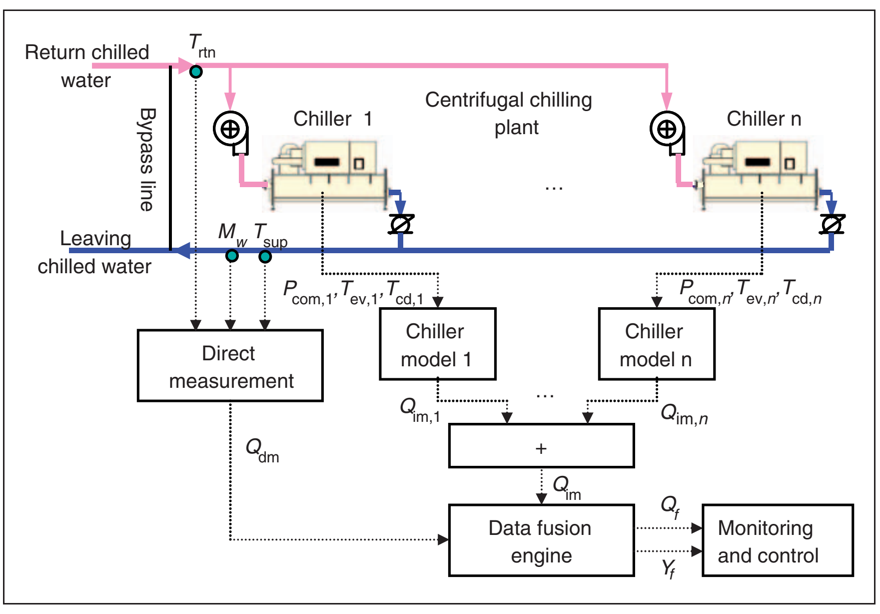

Figure 2. Schematic diagram of the chiller-model-based data fusion approach

where x_m is the fused measurement; x_i is the redundant measurement from the ith source; and $U_{i,k}$ is the uncertainty associated with x_i, which can be derived according to the standard derivation of the noises in x_i when the noises follow a normal distribution. Formula (12) is derived using the principle of maximum likelihood estimator (MSE).[20] For the cooling load measurement, the variable x could be the chilled water return temperature, the leaving temperature and the flow rate.

According to the theory of maximum likelihood estimator, the uncertainty associated with the fused measurements is calculated by

$$U_{f,k} = 1 \Bigg/ \sqrt{\sum_{i=0}^{M_k} \frac{1}{U_{i,k}^2}} \tag{13}$$

where $U_{i,k}$ is the uncertainty associated with the ith measurement and M_k is the number of redundant measurements. If M_k is larger, $U_{f,k}$ will be smaller. Therefore, more redundant measurements result in more accurate fused measurements.

Consider the case when the operating chillers can provide the real-time data of the chilled water return temperature, leaving temperature and flow rate. Without considering the heat loss from pipes, the actual values of the chilled water return temperature for the measurement at the header pipe and inside the operating chillers are the same. Therefore, the chilled water return temperature measurement has the form of Equation (14), which is redundant with the measurement described by Equation (2), because they share the same actual value $T_{\mathrm{rtn,act},k}$:

$$T_{\mathrm{rtn},i,k} = T_{\mathrm{rtn,act},k} + e_{\mathrm{rtn},i,k} + b_{\mathrm{rtn},i},\ e_{\mathrm{rtn},i} \sim N\left(0, \sigma_{\mathrm{rtn},i}^2\right) \tag{14}$$

where i is the ith operating chiller and $i = 1, \ldots, N$. Similarly, when the operating chillers have the same set point for the leaving temperature and the dynamics of the set point tracking are neglected, the chilled water leaving temperature can be written as Equation (15), which is redundant with the measurement described by Equation (3):

$$T_{\mathrm{lev},i,k} = T_{\mathrm{lev,act},k} + e_{\mathrm{lev},i,k} + b_{\mathrm{lev},i}\ e_{\mathrm{lev},i} \sim N\left(0, \sigma_{\mathrm{lev},i}^2\right). \tag{15}$$

For the chilled water flow rate, since the measurement at the header pipe is the total flow, the actual value of the total flow measurement should be equal to the sum of the actual values of the measurements provided by the operating chillers, that is,

$$\dot{m}_{\mathrm{act},k} = \sum_{i=1}^{N} \dot{m}_{\mathrm{act},i,k}. \tag{16}$$

Hence, the sum of the individual flow measurements provided by the operating chillers, which is calculated by Equation (17), is redundant with the measurement described by Equation (4):

$$\dot{m}_{w,\mathrm{tot},k} = \sum_{i=1}^{N} \dot{m}_{w,i,k} = \dot{m}_{w,\mathrm{act},k} + e_{w,\mathrm{tot},k} + b_{w,\mathrm{tot}} \tag{17}$$

where $\dot{m}_{w,i}$ is the flow measurement given by the ith operating chiller and has the form of

$$\dot{m}_{w,i} = \dot{m}_{w,\mathrm{act},i} + e_{w,i} + b_{w,i},\ e_{w,i} = N \sim \left(0, \sigma_{w,i}^2\right)$$

and $e_{w,\mathrm{tot},k}$ and $b_{w,\mathrm{tot}}$ are

$$e_{w,\mathrm{tot},k} \sim N\left(0, \sum_{i=1}^{N} \sigma_{w,i}^2\right),\ b_{w,\mathrm{tot}} = \sum_{i=1}^{N} b_{w,i}. \tag{18}$$

The structure of the MSF approach for the multiple-chiller plant is illustrated in Figure 3. The MSF approach has the functions of detecting and removing outliers in the redundant

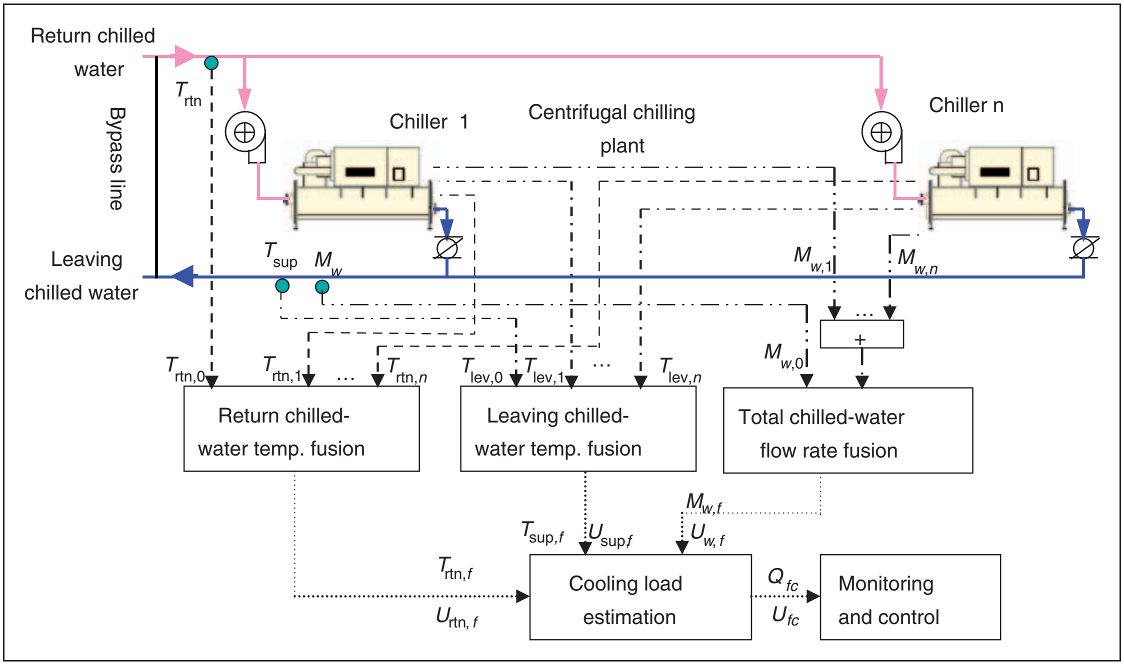

Figure 3. Schematic diagram of the multiple-sensor-based fusion approach

measurements, calibrating the bias the fused measurements and estimating the uncertainty associated with the fused measurement. The details are provided in Appendix B for self-consistency.

Comparison of the disciplines used in the two fusion approaches

The disciplines used in the two fusion approaches are summarised in Table 1 and the details are given in Appendix A and B. Table 1 shows that the two approaches use different disciplines to detect and remove outliers, reduce measurement noises and biases, and evaluate the quality of the fused measurements. Due to the difference, the two approaches have their own advantage and disadvantage under different operating conditions. Since the outlier and bias detection depends on user-specified parameters, only the basic fusion formula used in the two approaches is analysed.

Influence of cooling load dynamics

The cooling load dynamics affects the performance of the CMF approach because the error $\delta_{im,k}$ in Equation (9) (due to the model mismatch) has a different magnitude at different loads. The error can be efficiently removed by using the incremental form under the condition that the cooling load does not change significantly. However, if this condition is not satisfied, then the errors due to the model mismatch will be accumulated in the fused measurement, especially when a long moving window is used. Besides, the cooling load variation activates the dynamic behaviour between the chiller power consumption W_{ch} and the cooling load Q_{im}. When the cooling load has a rapid and large change, the power consumption will also vary considerably, but the variation in the power is not consistent with (usually lag behind) that of the cooling load. This inconsistency is not considered in the inverse chiller model. As a result,

Table 1. the disciplines used in the two fusion approaches

Functions	Chiller-model-based fusion approach	Multiple-sensor-based fusion approach
Reduce measurement noise	Construct the fused measurement using the sum of the direct measurements and the increments of the indirect measurements	Construct the fused measurement using maximum likelihood estimator
Detect/remove outlier	Compare the increment of the direct with that of the indirect measurement	Check consistency using the Moffat distance between redundant measurements
Reduce measurement bias	Compare the direct measurement with the fused measurement	Use bias shift technique
Evaluate the quality of the fused measurement	Calculate the confidence degree of the fused measurements	Calculate the uncertainty range of the fused measurements

the error $\delta_{\mathrm{im},k}$ may have a large magnitude during the transient and compromise the accuracy of the fused measurement.

The cooling load dynamics, on the other hand, has a much less influence on the performance of the MSF approach. This is because if the load varies, this variation will be measured by the temperature sensors whether located at the header pipes or inside the operating chillers.

Influence of the operating chiller number

The performance of the MSF approach will be mainly affected by the number of redundant measurements. When all the chillers in a chiller plant are able to provide the measurement of the chilled water return temperature and leaving temperature, more operating chillers will provide more redundant measurements on the chiller water return and leaving temperature. Hence, the accuracy of the fused chilled water return temperature and leaving temperature will be improved. However, there are only two redundant measurements for the chiller water flow rate regardless of the operating chiller number: one is measured from the header pipe and the other is the sum of the branch flow rate measured from the operating chillers. The uncertainty associated with the sum of the branch flow rates will increase when the operating chiller number becomes larger (see the definition of the standard deviation for $e_{w,\mathrm{tot},k}$ in Equation (18)). The accuracy of the flow rate may be reduced if more chillers are operating. Nevertheless, comparing with the accuracy improvement in the temperature measurement, the accuracy deterioration in the flow rate is less significant. This is because the rated temperature differential in Equation (1) usually has a small value and the temperature measurement uncertainties will have a larger influence on the accuracy of the cooling load calculation.[12] Therefore, the overall accuracy of the cooling load estimation using the fused measurement will still be improved.

On the other hand, the increase of the operating chiller number will usually decrease the accuracy of the CMF approach. Although the inverse chiller model for each chiller can be identified individually, the error $\delta_{\mathrm{im},k}$ will become larger (see Equation (9)) when the number of operating chillers increases. In this case, the CMF approach may suffer even more from the error $\delta_{\mathrm{im},k}$ due to the model mismatch.

Table 2. suggested application of the two fusion approach under different load condition

	Small number of operating chillers	Large number of operating chillers
Cooling load variation is significant	Both approaches may produceunsatisfactory result	The MSF approach is preferable
Cooling load variation is slight	The CMF approach is preferable	The MSF approach is preferable

Suggested applications of the two fusion approaches

As a summary, the performance of the two approaches will be different under different cooling load conditions. Their applications are suggested in Table 2. When redundant measurements are abundant, the MSF will be a good alternative; when redundant measurement is deficient and the cooling load is stable, the CMF will be a good alternative. In the case when the cooling load variation is significant and redundant measurements are not sufficient, both methods may produce an unsatisfactory estimation of the cooling load. However, the fused measurement from both approaches will still be better than the raw measurement by Equation (1).

One may suggest the integration of the two approaches, that is, to use the fused measurements from the MSF approach to replace the direct measurements in the CMF approach. However, this integration might not result in a noticeable improvement in the accuracy of the fused measurement in the CMF approach. This is because the accuracy of the CMF approach mainly depends on accuracy of the calibration part from the indirect measurement when the moving window is long.

Case study

Simulation platform of the multiple-chiller plant

A simulation study was conducted to validate the analysis on the comparison of the two fusion approaches in "Comparison of the disciplines used in the two fusion approaches". The simulation platform was constructed using TRNSYS 16. Six identical water-cooled centrifugal chillers were used and connected in a decoupled manner as shown in Figure 1. The rated capacity of each chiller was 7230 kW and each chiller was interlocked with a constant-speed pump with a designed flow rate of 345 l/s. The chillers and pumps were simulated using their dynamic physical models described in the study.[18] In the following study, the simulation platform was considered as an '*actual*' chiller plant.

The data generated from the constructed platform were used to identify the two parameters in the chiller model (7) for the CMF approach: the variable part α and the constant part of the electromechanical losses β. The data used for the identification covered the chiller load from 30% to 100%. Using the least square method, the parameters were identified as $\alpha = 0.882$ and $\beta = 381.2$ kW. Since identical chillers were used, the above α and β were applied to the model of each chiller.

Simulation of the measurement uncertainties

In order to make the comparison similar to real application, noises in the temperature and flow rate measurement were generated following the noises distribution derived from a sample of data using statistic tools. These data were collected from a chiller plant in a real building of Hong Kong, and the cooling capacity of each chiller was 7230 kW. Figure 4 shows the samples of the water temperature measurement and the water flow rate measurement. A norm

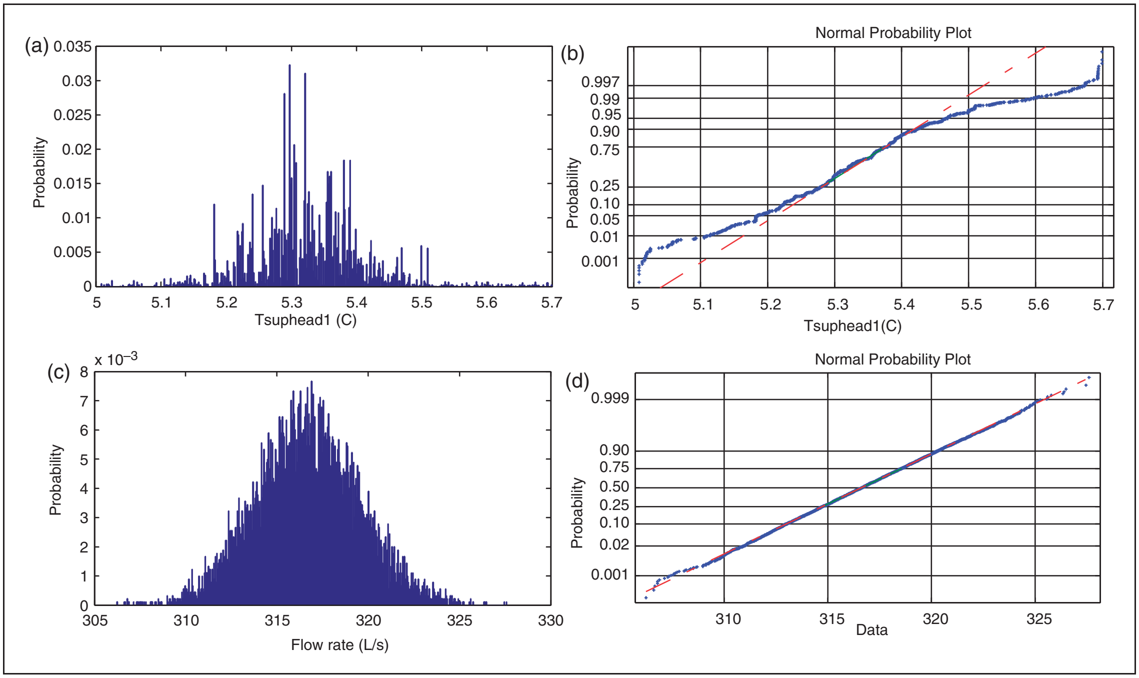

Figure 4. (a) the sample of the temperature measurements at the header pipe; (b) normal distribution test of the temperature measurements; (c) the sample of the water flow measurements at the header pipe; and (d) normal distribution test of the flow measurements

distribution test of the samples was performed in MATLAB using an integrated function NORMPLOT. The purpose of this function is to graphically assess whether the sample data could come from a normal distribution. The better the normal distribution is followed, the better the linearity of the dash-dotted line is. The result is shown in Figure 4, which indicates that those measurements follow well a normal distribution, especially the water flow measurement.

From the samples of the data, the standard deviations of the noises in the temperature and water flow measurements at the header pipe were derived. Similarly, the standard deviations of the noises in the temperature and water flow measurements provided by the chillers were also calculated using a sample of field data. Those standard deviations are listed in Table 3. With the standard deviation, the noises were produced using the function 'random' in MATLAB.

Results and analysis

The performance of the two approaches was firstly analysed using a typical spring day, during which one chiller can fulfil the cooling load demand. Figure 5(a) compares the cooling load raw estimation (which was calculated by Equation (1) without any fusion) with the cooling load actual value. It can be seen that the influence of measurement noises had a significant influence on the accuracy of the raw estimation. The raw estimations were very noisy. Figure 5(b) illustrates the comparison between the cooling load actual value and the indirect measurement calculated using the chiller inverse model (Eqnuations 7 and 8), which shows that

Table 3. Measurement uncertainties used in the case studies

	Standard deviation		
Sensor/meter location	Return temperature measurement (°C)	supply temperature measurements (°C)	Flow rate (*l/s*)
Header pipe	0.16	0.15	2
Chiller 1	0.15	0.15	1.5
Chiller 2	0.17	0.11	1.7
Chiller 3	0.15	0.13	1.8
Chiller 4	0.12	0.11	1
Chiller 5	0.11	0.12	2
Chiller 6	0.13	0.15	1.6

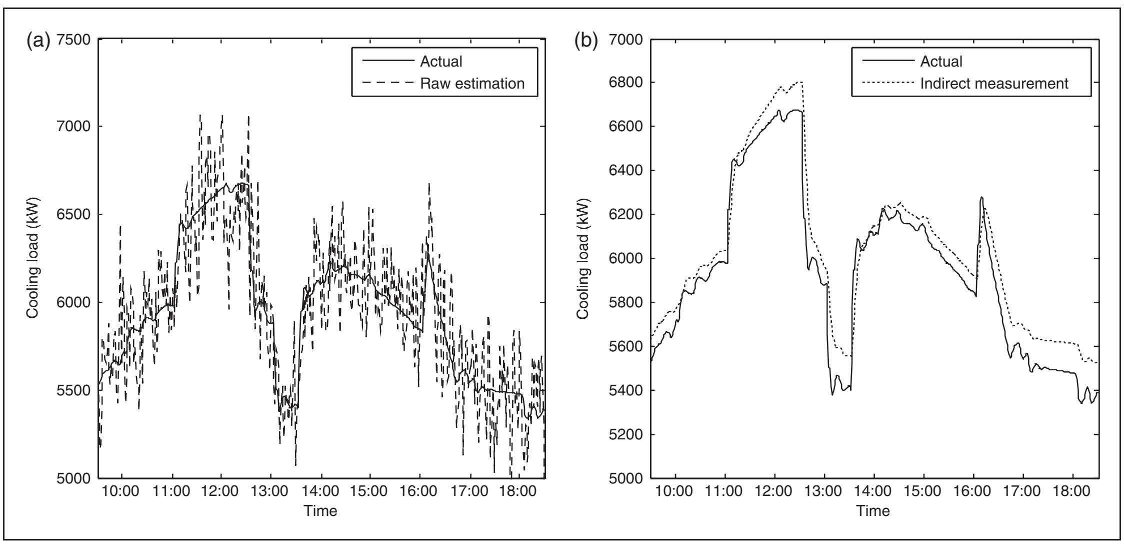

Figure 5. Cooling load in a typical spring day: (a) compare the raw estimation with the real value and (b) compare the indirect measurement with the real value

the chiller inverse model can estimate the cooling load but suffer from model mismatches.

Figure 6(a) compares the fused cooling load by the CMF approach with the actual cooling load and the differences between them are illustrated in Figure 6(b). Figure6(a) and (b) show that the cooling load fused estimation by the CMF approach was greatly improved compared with the raw estimation. Large difference mainly occurred when the cooling load had rapid changes as shown in Figure 6(a), for example during the period from 13:00 to 14:00 that was lunch time and during the period from 16:00 to 17:00 when a load spike was artificially added. The comparison between the actual cooling load and the fused load by the MSF approach was illustrated in Figure 6(c) and (d). Since one chiller was operating, there were only two

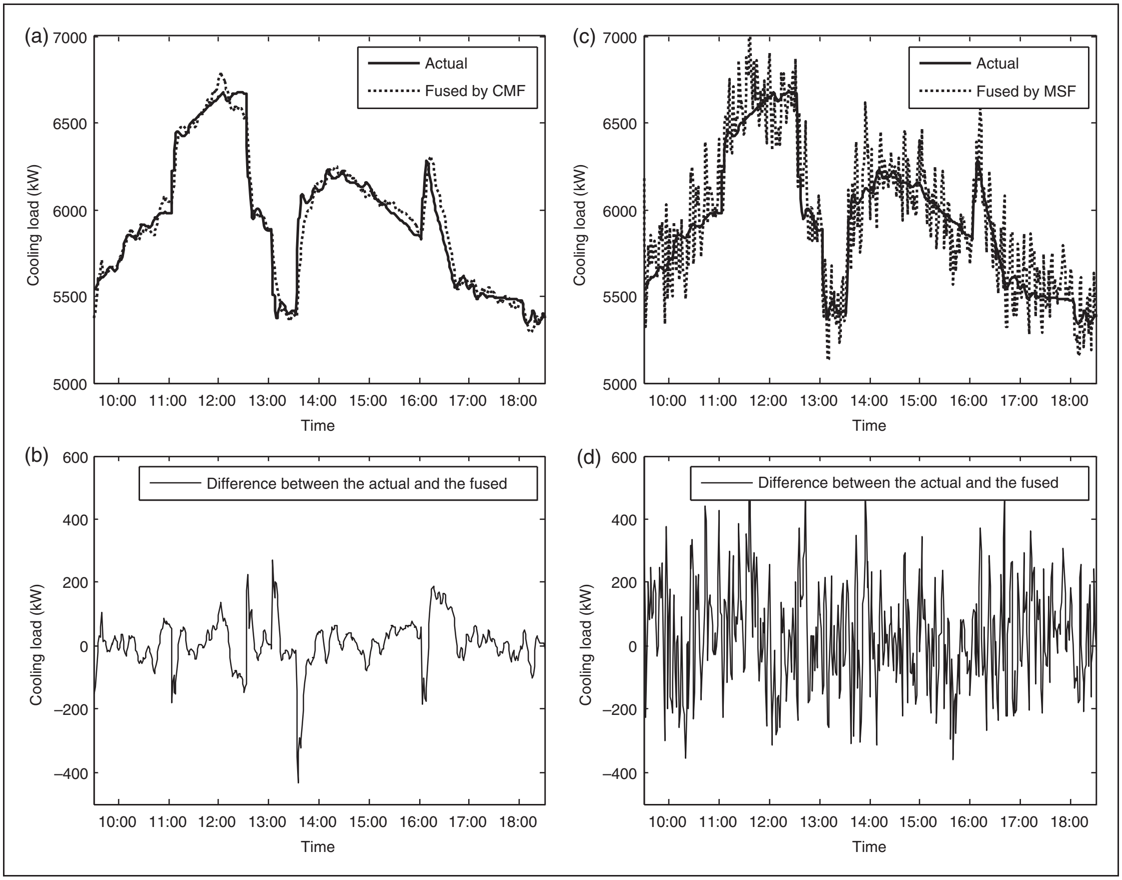

Figure 6. The performance of the two fusion approach in a typical spring day: (a) compare the CMF fused measurement with the actual value; (b) the difference between the CMF fused measurement and the actual value; (c) compare the MSF fused measurement with the actual value; and (d) the difference between the MSF fused measurement and the actual value

redundant measurements for the three measurements, respectively. Therefore, the improvement was not very obvious using the MSF approach. The root mean square errors (RMSE) of raw estimation, indirect measurement, CMF-fused measurement and the MSF fused measurement were 172, 99, 53 and 133 kW, respectively, which shows that in this example the CMF approach achieved the best accuracy.

The performance of the two approaches was also compared using an extremely hot summer day, during which six chillers were switched on to satisfy the cooling load demand. The comparison is illustrated by Figure 7. Figure 7(a) compares the fused cooling load by the CMF approach with the actual cooling load and Figure 7(b) illustrates the differences between them. Similar to the case with one chiller being operating, large difference occurred when the cooling load changed rapidly: for example, during the period from 12:00 to 13:00 and the period from 16:00 to 17:00. Figure 7(c) and 7(d) show the comparison between the fused load by the MSF approach and the actual cooling load. It can be seen that since more chillers were operating and more redundant

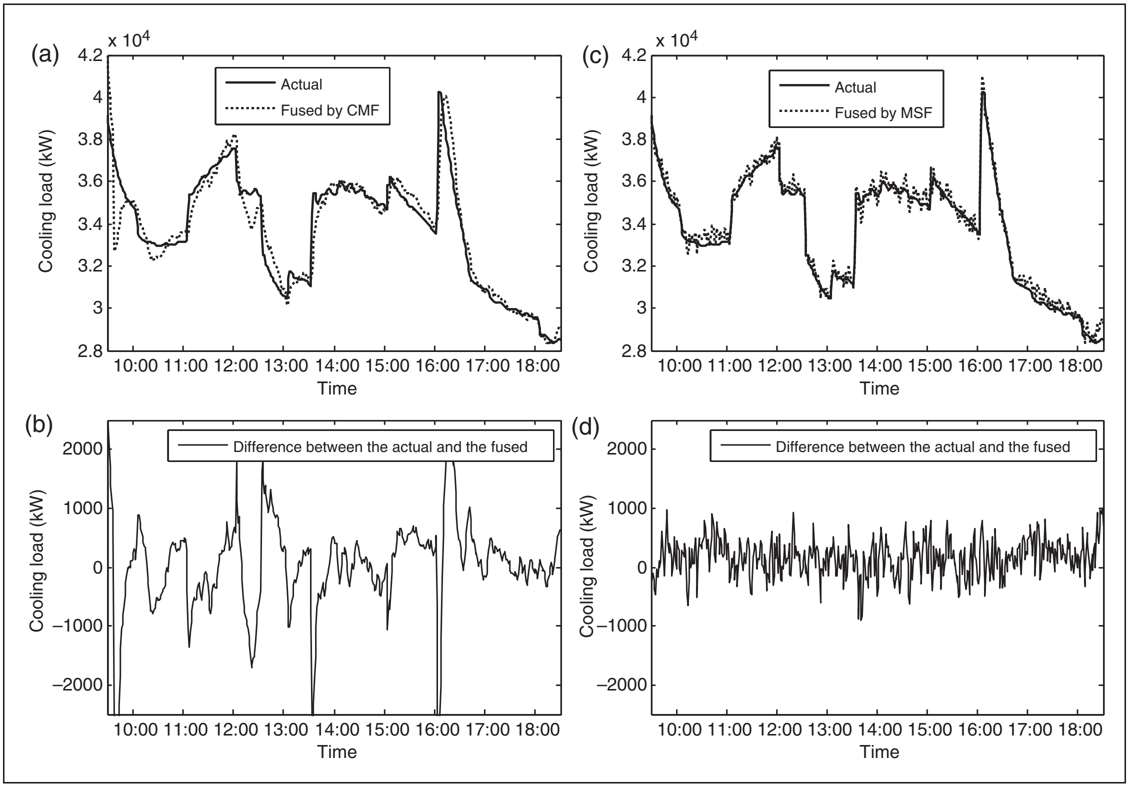

Figure 7. The performance of the two fusion approach in a hot summer day: (a) compare the CMF fused measurement with the actual value; (b) the difference between the CMF fused measurement and the actual value; (c) compare the MSF fused measurement with the actual value; and (d) the difference between the MSF fused measurement and the actual value

Table 4. RMSE comparison between the two fusion approaches with different number of operating chillers

	RMSE (kW)	
Number of operating chillers	The CMF approach	The MSF approach
1	53	133
2	259	189
3	329	235
4	369	249
5	443	267
6	669	286

measurements were available, the performance of the SMF approach became better. The RMSE of the CMF approach and the MSF approach were 669 and 286 kW, respectively, which shows that in this case the CMF approach achieved a better accuracy of the cooling load estimation.

An extended test was conducted to compare the RMSE of these two fusion approaches with chiller operating number varying from 1 to 6. The comparison result is shown in Table 4. The RMSE of the two approaches increased with the increase of the chiller operating number. However, the increase rates of the two approaches were different. When there were two or more chillers operating, the performance of the SMF approach was better than that of the CMF approach.

Conclusion

This paper has compared two fusion approaches that were developed to improve the accuracy of building instantaneous cooling load measurement using different disciplines. With the help of computer simulation, the paper shows that the two approaches have their own disadvantages and advantages under different load conditions. When redundant measurements are abundant which may happen when the cooling load is heavy and more chillers are operating, the MSF is a better alternative. When redundant measurement is deficient and the cooling load is stable that may happen when the cooling load is slight and one chiller is operating, the CMF is a better alternative. The selection of the fusion approach for practical applications should be helped by evaluating the cooling load condition of the chiller plants.

Funding

The Star-up Grant for New Staff, City University of Hong Kong.

Acknowledgement

The authors would like to thank for the funding support from the Start-up Grant for New Staff of the City University of Hong Kong (Project number: 7200176-BST).

Nomenclature

Q	building cooling load (kW)
$\dot{m}$	mass flow rate (L/s)
b	bias
cp_g	gaseous refrigerant specific heat at a constant pressure (kJ/k·kg)
cp_l	liquid refrigerant specific heat at a constant pressure (kJ/k·kg)
h_{fg}	the latent heat at reference state pressure (kJ/kg)
P	pressure (Pa)
U	uncertainty
T	temperature (°C)
e	noises
W	power consumption (kW)
r	refrigerant gas constant (J/K·kg·s)
rtn	return
lev	leaving
w	chilled water
hd	variable measurement at header pipes
k	time instant
act	actual value
im	indirect measurement
dm	direct measurement
cd	condensing
ev	evaporating
ρ	specific heat capacity (J/K·kg)
σ	standard deviation
α	variable part of the compressor electromechanical loss
β	constant part of compressor electromechanical loss (kW)
γ	polytropical compressor coefficient
ζ	refrigerant gas compressor coefficient
δ	measurement error due to model mismatch (kW)

References

1. Honeywell. *Engineering manual of automatic control for commercial buildings*. Multiple Chiller System Control Applications. Minneapolis, MN: Honeywell SI Edition, 1997, pp.308–315.
2. ASHRAE. ASHRAE handbook of applications. In: Noble RE (ed.) *Supervisory control strategies and optimization*. Atlanta, GA: ASHRAE, 2011, pp.42.1–42.44.
3. Huang GS, Wang SW and Sun YJ. Enhancing the reliability of chiller control using fused measurement of building cooling load. *HVAC&R Research* 2008; 14(6): 941–958.
4. Ardehali MM and Smith TF. Evaluation of HVAC system operational strategies for commercial buildings. *Energy Conversion and Management* 1997; 38: 225–236.
5. Wang SW and Wang JB. Law-based sensor fault diagnosis and validation for building air-conditioning systems. *HVAC&R Research* 1999; 5: 353–380.
6. Dossat RJ. *Principles of refrigeration*. Cooling Load Calculations. Chapter 10. New York: Wiley, 1991, pp.163–198.

7. Kwan C (2001). Investigation of sensor topology for sequential control of chiller plants for efficient operation and control. MSc Dissertation, Department of Building Services Engineering, Hong Kong Polytechnic University, 2001.
8. Stum K. Sensor accuracy and calibration theory and practical application. *Proceeding of National Conference on Building Commissioning*. San Francisco, USA April 19–21, 2006. Available at: http://www.peci.org/ncbc/proceedings/2006/index.htm.
9. Taylor Engineering, Chilled water plant design guideline. 2009. Available at: http://www.taylor-engineering.com/
10. Strunz T, Wiest A, Fleury A, Fröhlich T. *Influence of turbulence on ultrasonic flow measurements, the fifth IGHEM conference*. Lucerne, Switzerland, from July 14–16, 2004. Available at: http://www.ighem.org/
11. Hofmann F. *Fundamental principles of electromagnetic measurement*, 3rd edn. Chapter 6. Duisburg: KROHNE Messtechnik GmbH & Co. KG, 2003, pp.52–57.
12. Huang GS, Wang SW, Xiao F and Sun YJ. A data fusion scheme for building automation systems of building central chilling plants. *Automation in Construction* 2009; 18: 302–309.
13. Salsbury TI. A survey of control technologies in the building automation industry. *Proceedings of the 16th IFAC world congress*. Czech Republic: Prague, 2005: 331–341.
14. Natori K, Oboe R and Ohnishi K. Stability analysis and practical design procedure of time delayed control systems with communication disturbance observer. *IEEE Transactions on Industrial Informatics* 2008; 4: 185–197.
15. Huang GS, Wang SW and Xu XH. Robust model predictive control of VAV air-handling units concerning uncertainties and constraints. *HVAC&R Research* 2010; 16(1): 15–33.
16. Huang GS, Sun YJ and Li P. Fusion of redundant measurements for enhancing the reliability of total cooling load-based chiller sequencing control. *Automation in Construction* 2011; 20: 789–798.
17. TRNSYS, TRANSYS 16 documentation. 2004. http://sel.me.wisc.edu/trnsys.
18. Wang SW, Wang JB and Burnett J. Mechanistic model of centrifugal chillers for HVAC system dynamics simulation. *Building Services Engineering Research and Technology* 2000; 21: 73–83.
19. Browne MW and Bansal PK. steady-state model of centrifugal liquid chillers. *International Journal of Refrigeration* 1998; 21: 343–358.
20. Ozyurt DB and Pike RW. Theory and practice of simultaneous data reconciliation and gross error detection for chemical process. *Computer and Chemical Engineering* 2004; 28: 381–402.

Appendix A: the chiller-model-based fusion algorithm

The fusion algorithm follows the procedure illustrated in Figure A1. A moving window is used in the fusion algoritm. The moving window is defined as a table with a horizon of N samples, and it stores two groups of data. Group 1 consists of N direct measurements w and Group 2 consists of the corresponding (measured at the same time) indirect measurements. Using the superscript κ to indicate the data at the current moving window and the data in the moving window are

$$\text{Group1}: Q^{\kappa}_{\text{dm},1}, \ldots, Q^{\kappa}_{\text{dm},N} \quad \text{Group2}: Q^{\kappa}_{\text{im},1}, \ldots, Q^{\kappa}_{\text{im},N}.$$

Following the flowchart, the fusion algorithm of the chiller-model-based fusion approach is described as below.

To detect and remove outlier: the current direct measurement $Q_{\text{dm},k}$ is detected as an outlier if d_k, defined by Equation (A1), is larger than a threshold E_m, where the threshold E_m is an user-dependent parameter, where $\Delta Q_{\text{dm},k} = Q_{\text{dm},k} - Q_{\text{dm},k-1}$ and $\Delta Q_{\text{im},k} = Q_{\text{im},k} - Q_{\text{im},k-1}$. In this case, the fused measurement is given by Equation (A2) and the confidence degree is calculated by Equation (A3). Equation (13) indicates that the confidence degree decays in a rate of β_1 in the case of outliers:

$$d_{\Delta,k} = \Delta Q_{\text{dm},k} - \Delta Q_{\text{im},k} \tag{A1}$$

$$Q_{f,k} = Q_{f,k-1} + \Delta Q_{\text{im},k} \tag{A2}$$

$$\gamma_{f,k} = \beta_1 \gamma_{f,k-1}. \tag{A3}$$

To update the moving window: the moving window will be updated only if the current direct measurement $Q_{\text{im},k}$ is not detected as an

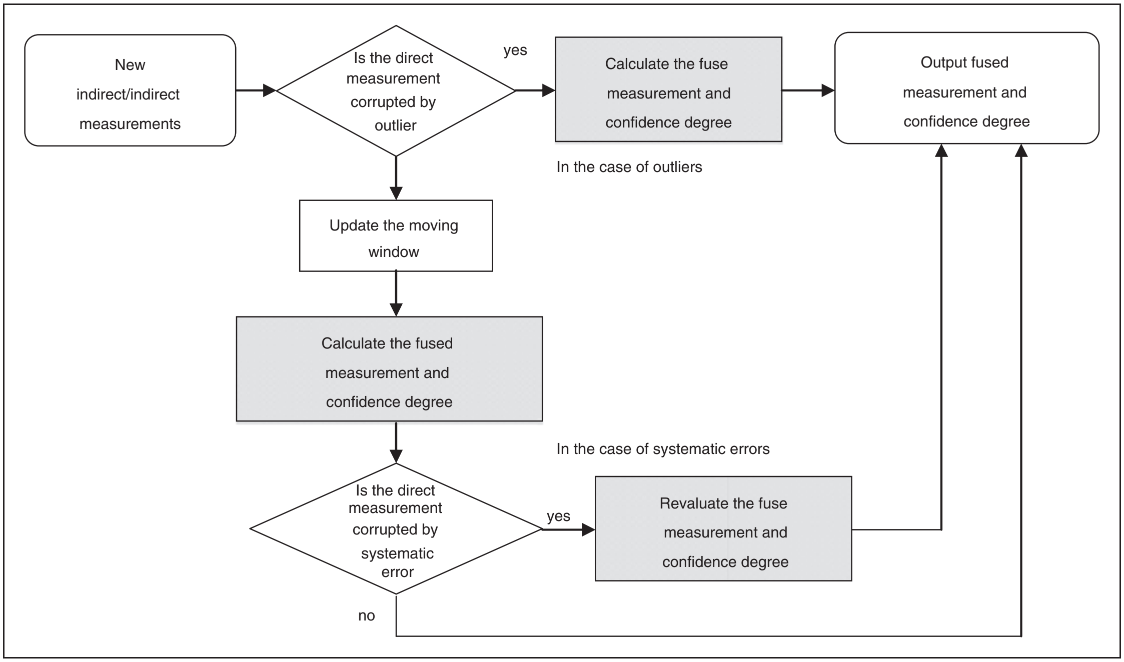

Figure A1 Flowchart of the chiller-model-based fusion algorithm

outlier. It is updated by Equation (A4) where $i = 1, \ldots, N$ and by Equation (A5):

$$Q^{\kappa}_{\mathrm{dm},\,i} = Q^{\kappa}_{\mathrm{dm},\,i+1}, Q^{\kappa}_{\mathrm{im},\,i} = Q^{\kappa}_{\mathrm{im},\,i+1} \tag{A4}$$

$$Q^{\kappa}_{\mathrm{dm},\,N} = Q_{\mathrm{dm},\,k}, Q^{\kappa}_{\mathrm{im},\,N} = Q_{\mathrm{im},\,k}. \tag{A5}$$

To fuse the indirect and direct measurements: the fused measurement is constructed by Equation (10). The confidence degree is calculated by Equation (A6), which indicates that without systematic error the confidence degree is larger than β_1:

$$\gamma_{f,k} = 1 - (1 - \beta_1) \frac{\left|\sum_{i=2}^{N} \left|\Delta Q^{\kappa}_{\mathrm{im},\,i}\right| - \sum_{i=2}^{N} \left|Q^{\kappa}_{\mathrm{dm},\,i} - Q^{\kappa}_{\mathrm{dm},\,i-1}\right|\right|}{(N-1) \times E_m}. \tag{A6}$$

To detect a large bias: the differential between the fused measurement calculated by Equation (10) and the current direct measurement $Q_{\mathrm{dm},k}$ is used to detect a large bias in the direct measurement. If the differential is inside a predefined range, that is, $[E_L, E_U]$, no bias is detected and the fused measurement by Equation (10) and the confidence degree by Equation (A6) will be output as the final fused value and the final confidence degree. Otherwise, a large bias in the direct measurements is believed to occur, and the fused measurement and the associated confidence degree will be revaluated.

To remove the influence of large bias: when a large bias is detected, the fused measurement is given by Equation (A7) and the confidence is calculated by Equation (A8), where β_2 is smaller than β_1 in order to distinguish systematic errors from outliers:

$$Q_{f,k} = Q_{\mathrm{im},\,k-1} + (E_L + E_U)/2 \tag{A7}$$

$$\gamma_{f,k} = \beta_2 \gamma_{f,k-1}. \tag{A8}$$

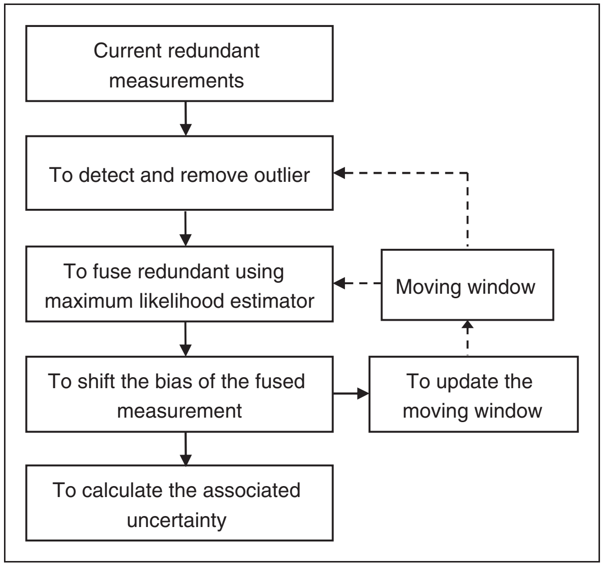

Figure B1 Flowchart of the multiple-chiller-based fusion algorithm

Appendix B: Multiple-sensor-based fusion algorithm

The fusion algorithms for the chilled water return temperature, leaving temperature and the flow rate follow the same procedure, which are shown in Figure B1. In the fusion algorithm, a moving window is also used, which stores previous measurements and provides data for applications in the outlier removal and bias calibration. The moving window is defined as a matrix with dimension $L_w \times N_r$, where L_w is called the length of the moving window and N_r is the number of redundant measurements. $x_1, \ldots, x_n$ are used to denote the redundant measurements, which have the following uncertainty form at the time instant k:

$$x_{i,k} = x_{\mathrm{act},k} + e_{i,k} + b_i \text{ with } e_i \sim N\left(0, \delta^2\right).$$

The fusion algorithm is described as follows.

To detect and remove outlier in redundant measurements: at each sampling time, a measurement is detected as an outlier if it is not mutually consistency with other measurements. The consistency is checked using Moffat distance between measurements, which is defined by Equation (B1), where $\bar{b}_{j,i,k}$ is an estimation of $(b_j - b_i)$ at the current time instant k. $\bar{b}_{j,i,k}$ is calculated by Equation (B2) using the data stored in the moving window. The details on the consistency are referred to in the study.[16] If a measurement is detected as an outlier, it will be discarded in the following fuse operation. The outputs of the outlier removal algorithm are the measurements that are mutually consistent as well as the associated calibrated uncertainty indices $U_{i,k}$:

$$d_{i,j,k} = \frac{\left| x_{i,k} - x_{j,k} + \bar{b}_{ji.k} \right|}{1.96\sqrt{\delta_i^2 + \delta_j^2}} \tag{B1}$$

$$\bar{b}_{\mathrm{ji},k} = \frac{1}{L_w} \sum_{t=L_w}^{1} \left(x_{j,t} - x_{i,t} \right). \tag{B2}$$

To fuse the redundant measurements using maximum likelihood estimation: after removing outliers, Equation (12) is used to calculate the fused measurements from the mutually consistent measurements.

To schedule the basis of the merged measurement: when a measurement with the smallest bias is known, the bias of the fused measurement is calibrated to the bias of that measurement. Using h to denote this measurement, the calibration is done by Equation (B3), where $\bar{b}_{h,i,k}$ is calculated by Equation (B4):

$$x_{f,k} = x_{m,k} + \sum_{i=0,\, i \neq h}^{M_k} \lambda_{i,k} \left(\bar{b}_{h,i,k} \right) \tag{B3}$$

$$\bar{b}_{h,i,k} = \frac{1}{L_w} \sum_{t=L_w}^{1} \left(x_{h,t} - x_{i,t} \right). \tag{B4}$$

To update of the moving window: at each sampling time, if there is no outlier found in the measurements, then update the ith row by the measurements stored in the (i−1)st row from $i = L_w$ to 1; and current measurements are placed into the first row; otherwise, no update is taken.

To calculate the associated uncertainty: the uncertainty associated with the fused measurement is given by Equation (13).